Laplacian Eigenfunctions That Do Not Feel the Boundary: Theory, Computation, & Applications

Naoki Saito

Department of Mathematics
University of California, Davis

Symposium on Geometry Processing
Lyon, France
July 5, 2010

Outline

Outline

Acknowledgment

- Faisal Beg & Pradeep Kumar (Simon Fraser Univ.)
- Raphy Coifman & Peter Jones (Yale)
- Dave Donoho (Stanford)
- Lotfi Hermi (Univ. Arizona)
- John Hunter (UCD)
- Hrushikesh Mhaskar (Cal State Univ. LA)
- Allen Xue (formerly UCD; currently Amgen Inc.)
- NSF
- ONR

Outline

Motivations

- Consider a bounded domain of general (may be quite complicated) shape $\Omega \subset \mathbb{R}^d$.
- Want to analyze the spatial frequency information inside of the object defined in $\Omega \Longrightarrow$ need to avoid the Gibbs phenomenon due to $\Gamma = \partial\Omega$.
- Want to represent the object information efficiently for analysis, interpretation, discrimination, etc. $\Longrightarrow$ fast decaying expansion coefficients relative to a meaningful basis.
- Want to extract geometric information about the domain $\Omega \Longrightarrow$ shape clustering/classification.

Motivations . . . Data Analysis on a Complicated Domain

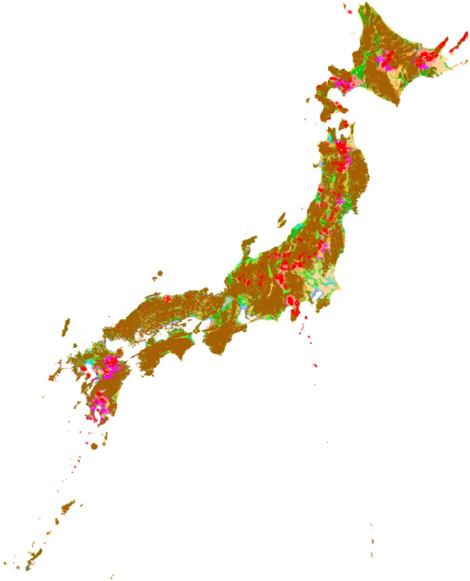

Outline

Eigenfunctions of Laplacian

- Our previous attempt was to extend the object to the outside smoothly and then bound it nicely with a rectangular box followed by the ordinary Fourier analysis.
- Why not analyze (and synthesize) the object using genuine basis functions tailored to the domain?
- After all, *sines* (and *cosines*) are the eigenfunctions of the Laplacian on the *rectangular* domain with Dirichlet (and Neumann) boundary condition.
- *Spherical harmonics, Bessel functions, and Prolate Spheroidal Wave Functions*, are part of the eigenfunctions of the Laplacian (via separation of variables) for the *spherical, cylindrical, and spheroidal* domains, respectively.

Eigenfunctions of Laplacian . . .

- Consider an operator $\mathcal{L} = -\Delta$ in $L^2(\Omega)$ with *appropriate* boundary condition.
- Analysis of $\mathcal{L}$ is difficult due to unboundedness, etc.
- Much better to analyze its inverse, i.e., the Green's operator because it is compact and self-adjoint.
- Thus $\mathcal{L}^{-1}$ has discrete spectra (i.e., a countable number of eigenvalues with finite multiplicity) except 0 spectrum.
- $\mathcal{L}$ has a complete orthonormal basis of $L^2(\Omega)$, and this allows us to do eigenfunction expansion in $L^2(\Omega)$.

Eigenfunctions of Laplacian . . . Difficulties

- The key difficulty is to compute such eigenfunctions; directly solving the Helmholtz equation (or eigenvalue problem) on a general domain is tough.
- Unfortunately, computing the Green's function for a general Ω satisfying the usual boundary condition (i.e., Dirichlet, Neumann) is also very difficult.

Outline

Integral Operators Commuting with Laplacian

- The key idea is to find an integral operator commuting with the Laplacian without imposing the strict boundary condition a priori.
- Then, we know that the eigenfunctions of the Laplacian is the same as those of the integral operator, which is easier to deal with, due to the following

Theorem (G. Frobenius 1896?; B. Friedman 1956)

Suppose $\mathcal{K}$ and $\mathcal{L}$ commute and one of them has an eigenvalue with finite multiplicity. Then, $\mathcal{K}$ and $\mathcal{L}$ share the same eigenfunction corresponding to that eigenvalue. That is, $\mathcal{L}\varphi = \lambda\varphi$ and $\mathcal{K}\varphi = \mu\varphi$.

- Let's replace the Green's function $G(\mathbf{x}, \mathbf{y})$ by the fundamental solution of the Laplacian:

$$K(\mathbf{x}, \mathbf{y}) = \begin{cases} -\frac{1}{2}|x - y| & \text{if } d = 1, \\ -\frac{1}{2\pi} \log |\mathbf{x} - \mathbf{y}| & \text{if } d = 2, \\ \frac{|\mathbf{x}-\mathbf{y}|^{2-d}}{(d-2)\omega_d} & \text{if } d > 2, \end{cases}$$

  where $\omega_d \triangleq \frac{2\pi^{d/2}}{\Gamma(d/2)}$ is the surface area of the unit ball in $\mathbb{R}^d$, and $|\cdot|$ is the standard Euclidean norm.
- The price we pay is to have rather implicit, non-local boundary condition although we do not have to deal with this condition directly.

Integral Operators Commuting with Laplacian . . .

- Let $\mathcal{K}$ be the integral operator with its kernel $K(\mathbf{x}, \mathbf{y})$:

$$\mathcal{K}f(\mathbf{x}) \triangleq \int_\Omega K(\mathbf{x}, \mathbf{y}) f(\mathbf{y}) \, \mathrm{d}\mathbf{y}, \quad f \in L^2(\Omega).$$

Theorem (NS 2005)

The integral operator $\mathcal{K}$ commutes with the Laplacian $\mathcal{L} = -\Delta$ with the following non-local boundary condition:

$$\int_\Gamma K(\mathbf{x}, \mathbf{y}) \frac{\partial \varphi}{\partial \nu_\mathbf{y}}(\mathbf{y}) \, \mathrm{d}s(\mathbf{y}) = -\frac{1}{2}\varphi(\mathbf{x}) + \operatorname{pv}\int_\Gamma \frac{\partial K(\mathbf{x}, \mathbf{y})}{\partial \nu_\mathbf{y}} \varphi(\mathbf{y}) \, \mathrm{d}s(\mathbf{y}),$$

for all $\mathbf{x} \in \Gamma$, where φ is an eigenfunction common for both operators.

Corollary (NS 2009)

The eigenfunction $\varphi(\mathbf{x})$ *of the integral operator* $\mathcal{K}$ *in the previous theorem can be extended outside the domain* Ω *and satisfies the following equation:*

$$-\Delta\varphi = \begin{cases} \lambda\,\varphi & \text{if } \mathbf{x} \in \Omega; \\ 0 & \text{if } \mathbf{x} \in \mathbb{R}^d \setminus \overline{\Omega}, \end{cases}$$

with the boundary condition that φ *and* $\dfrac{\partial\varphi}{\partial\nu}$ *are continuous across the boundary* Γ*. Moreover, as* $|\mathbf{x}| \to \infty$, $\varphi(\mathbf{x})$ *must be of the following form:*

$$\varphi(\mathbf{x}) = \begin{cases} \mathrm{const} \cdot |\mathbf{x}|^{2-d} + O\left(|\mathbf{x}|^{1-d}\right) & \text{if } d \neq 2; \\ \mathrm{const} \cdot \ln|\mathbf{x}| + O\left(|\mathbf{x}|^{-1}\right) & \text{if } d = 2. \end{cases}$$

Integral Operators Commuting with Laplacian . . .

Corollary (NS 2005)

The integral operator $\mathcal{K}$ is compact and self-adjoint on $L^2(\Omega)$. Thus, the kernel $K(\mathbf{x}, \mathbf{y})$ has the following eigenfunction expansion (in the sense of mean convergence):

$$K(\mathbf{x}, \mathbf{y}) \sim \sum_{j=1}^{\infty} \mu_j \varphi_j(\mathbf{x}) \overline{\varphi_j(\mathbf{y})},$$

and $\{\varphi_j\}_j$ forms an orthonormal basis of $L^2(\Omega)$.

Outline

Connection with Potential Theory

- Mark Kac mentioned at the very end of his 1951 paper (Proceedings of the 2nd Berkeley Symposium on Mathematical Statistics and Probability) that the same integral equation in 3D is equivalent to the Laplacian eigenvalue problem. But his boundary condition was not correct.
- In 1967–9, John Troutman studied the eigenvalues of the same integral operator (i.e., the logarithmic potential) in 2D. He posed this problem as the Laplacian eigenvalue problem whose eigenfunctions are harmonic outside of the given domain. He proved that there exists one negative eigenvalue iff the transfinite diameter (or logarithmic capacity) of the closed domain $\bar{\Omega}$ exceeds 1.
- In 1970, Mark Kac and Tomasz Bojdecki obtained similar results using probabilistic argument (Kac) and purely analytic method (Bojdecki).

Outline

1D Example

- Consider the unit interval $\Omega = (0, 1)$.
- Then, our integral operator $\mathcal{K}$ with the kernel $K(x, y) = -|x - y|/2$ gives rise to the following eigenvalue problem:

$$-\varphi'' = \lambda\varphi, \quad x \in (0, 1);$$

$$\varphi(0) + \varphi(1) = -\varphi'(0) = \varphi'(1).$$

- The kernel $K(\mathbf{x}, \mathbf{y})$ is of Toeplitz form $\Longrightarrow$ Eigenvectors must have even and odd symmetry (Cantoni-Butler '76).
- In this case, we have the following explicit solution.

1D Example . . .

- $\lambda_0 \approx -5.756915$, which is a solution of $\tanh \frac{\sqrt{-\lambda_0}}{2} = \frac{2}{\sqrt{-\lambda_0}}$,

$$\varphi_0(x) = A_0 \cosh \sqrt{-\lambda_0} \left(x - \frac{1}{2} \right);$$

- $\lambda_{2m-1} = (2m-1)^2\pi^2, \; m = 1, 2, \ldots,$

$$\varphi_{2m-1}(x) = \sqrt{2} \cos(2m-1)\pi x;$$

- $\lambda_{2m}, \; m = 1, 2, \ldots,$ which are solutions of $\tan \frac{\sqrt{\lambda_{2m}}}{2} = -\frac{2}{\sqrt{\lambda_{2m}}}$,

$$\varphi_{2m}(x) = A_{2m} \cos \sqrt{\lambda_{2m}} \left(x - \frac{1}{2} \right),$$

where $A_k, \; k = 0, 1, \ldots$ are normalization constants.

First 5 Basis Functions

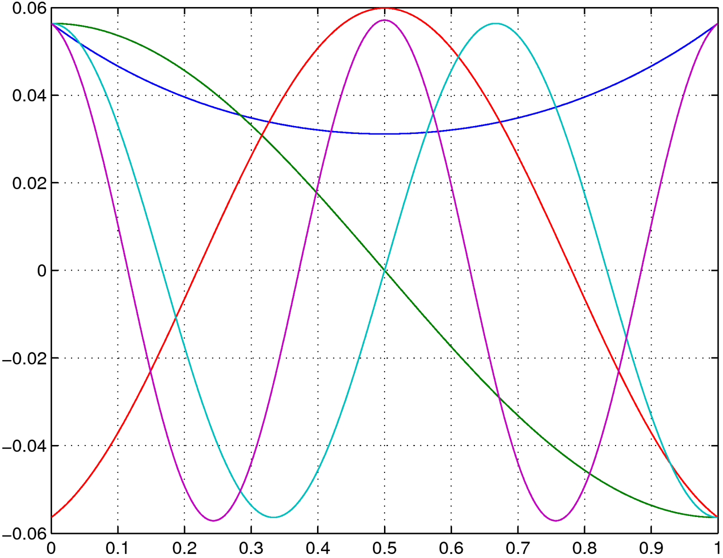

1D Example: Comparison

- The Laplacian eigenfunctions with the Dirichlet boundary condition: $-\varphi'' = \lambda\varphi$, $\varphi(0) = \varphi(1) = 0$, are *sines*. The Green's function in this case is:
$$G_D(x, y) = \min(x, y) - xy.$$
- Those with the Neumann boundary condition, i.e., $\varphi'(0) = \varphi'(1) = 0$, are *cosines*. The Green's function is:
$$G_N(x, y) = -\max(x, y) + \frac{1}{2}(x^2 + y^2) + \frac{1}{3}.$$
- Remark: Gridpoint $\Leftrightarrow$ DST-I/DCT-I;
Midpoint$\Leftrightarrow$ DST-II/DCT-II.

1D Example: Rayleigh Functions/Trace Formula

Corollary (NS 2008)

Let $\{\lambda_n\}_{n=0}^{\infty}$ *be the 1D Laplacian eigenvalues of the non-local boundary problem with the commuting integral operator whose kernel is* $K(x, y) = -|x - y|/2$. *Then, they satisfy the following trace formula:*

$$\sum_{n=0}^{\infty} \frac{1}{\lambda_n} = \int_0^1 K(x, x)\,\mathrm{d}x = 0.$$

Compare this with the famous Basel problem, which is based on the Dirichlet boundary condition:

$$\sum_{n=1}^{\infty} \frac{1}{\pi^2 n^2} = \int_0^1 G_D(x, x)\,\mathrm{d}x = \frac{1}{6} \quad \Longleftrightarrow \quad \sum_{n=1}^{\infty} \frac{1}{n^2} = \frac{\pi^2}{6}.$$

Theorem (NS 2008)

Let $K_p(x,y)$ be the pth iterated kernel of $K(x,y) = -|x-y|/2$. Then,

$$\sum_{n=0}^{\infty} \frac{1}{\lambda_n^p} = \int_0^1 K_p(x,x)\,\mathrm{d}x = \frac{1}{4^p}\left(S_{2p} + \frac{(-1)^p}{\alpha^{2p}}\right) + \frac{4^p-1}{2\cdot(2p)!}|B_{2p}|,$$

where $\alpha \approx 1.19967864$ *satisfies* $\alpha = \coth\alpha$, B_{2p} *is the Bernoulli number, and*

$$S_{2p} \triangleq \sum_{m=1}^{\infty}\left(\frac{4}{\lambda_{2m}}\right)^p,$$

satisfies the following recursion formula:

$$\sum_{\ell=1}^{n+1} \frac{(-1)^{n-\ell+1}\left(2\left(n-\ell+1\right)-1\right)}{\left(2\left(n-\ell+1\right)\right)!}\left\{S_{2\ell} + \frac{(-1)^{\ell}}{\alpha^{2\ell}}\right\} = \frac{(-1)^n}{2(2n)!}.$$

2D Example

- Consider the unit disk Ω. Then, our integral operator $\mathcal{K}$ with the kernel $K(\mathbf{x}, \mathbf{y}) = -\frac{1}{2\pi} \log |\mathbf{x} - \mathbf{y}|$ gives rise to:

$$-\Delta\varphi = \lambda\varphi, \quad \text{in } \Omega;$$
$$\left.\frac{\partial\varphi}{\partial\nu}\right|_\Gamma = \left.\frac{\partial\varphi}{\partial r}\right|_\Gamma = -\left.\frac{\partial\mathcal{H}\varphi}{\partial\theta}\right|_\Gamma,$$

  where $\mathcal{H}$ is the Hilbert transform for the circle, i.e.,

$$\mathcal{H}f(\theta) \triangleq \frac{1}{2\pi}\ \mathrm{pv}\int_{-\pi}^{\pi} f(\eta) \cot\left(\frac{\theta-\eta}{2}\right) \mathrm{d}\eta \quad \theta \in [-\pi, \pi].$$

- Let $\beta_{k,\ell}$ is the ℓth zero of the Bessel function of order k, $J_k(\beta_{k,\ell}) = 0$. Then,

$$\varphi_{m,n}(r,\theta) = \begin{cases} J_m(\beta_{m-1,n}\, r)\binom{\cos}{\sin}(m\theta) & \text{if } m = 1, 2, \ldots,\ n = 1, 2, \ldots, \\ J_0(\beta_{0,n}\, r) & \text{if } m = 0,\ n = 1, 2, \ldots, \end{cases}$$

$$\lambda_{m,n} = \begin{cases} \beta^2_{m-1,n}, & \text{if } m = 1, \ldots,\ n = 1, 2, \ldots, \\ \beta^2_{0,n} & \text{if } m = 0,\ n = 1, 2, \ldots. \end{cases}$$

First 25 Basis Functions

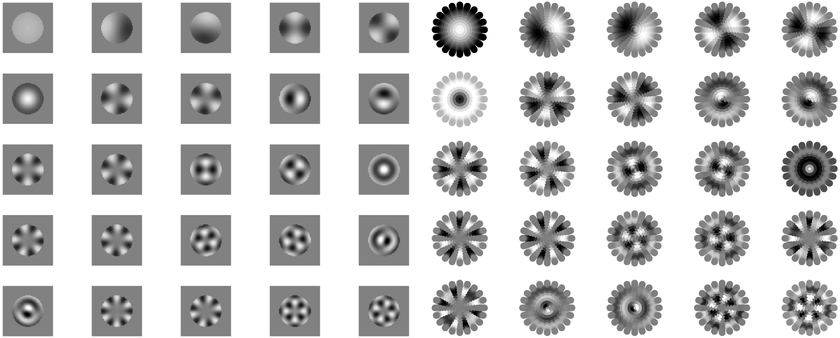

(a) Our Basis (b) Dirichlet-Laplace

3D Example

- Consider the unit ball Ω in $\mathbb{R}^3$. Then, our integral operator $\mathcal{K}$ with the kernel $K(\mathbf{x}, \mathbf{y}) = \frac{1}{4\pi|\mathbf{x}-\mathbf{y}|}$.
- Top 9 eigenfunctions cut at the equator viewed from the south:

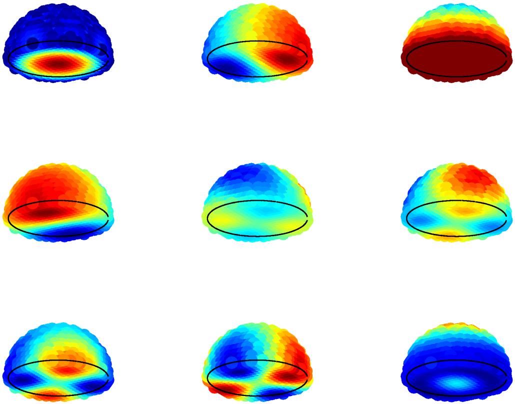

Outline

Discretization of the Problem

- Assume that the whole dataset consists of a collection of data sampled on a regular grid, and that each sampling cell is a box of size $\prod_{i=1}^{d} \Delta x_i$.
- Assume that an object of our interest Ω consists of a subset of these boxes whose centers are$\{\mathbf{x}_i\}_{i=1}^{N}$.
- Under these assumptions, we can approximate the integral eigenvalue problem $\mathcal{K}\varphi = \mu\varphi$ with a simple quadrature rule with node-weight pairs $(\mathbf{x}_j, w_j)$ as follows.

$$\sum_{j=1}^{N} w_j K(\mathbf{x}_i, \mathbf{x}_j)\varphi(\mathbf{x}_j) = \mu\varphi(\mathbf{x}_i), \quad i = 1, \ldots, N, \quad w_j = \prod_{i=1}^{d} \Delta x_i.$$

- Let $K_{i,j} \triangleq w_j K(\mathbf{x}_i, \mathbf{x}_j)$, $\varphi_i \triangleq \varphi(\mathbf{x}_i)$, and $\boldsymbol{\varphi} \triangleq (\varphi_1, \ldots, \varphi_N)^T \in \mathbb{R}^N$. Then, the above equation can be written in a matrix-vector format as: $K\boldsymbol{\varphi} = \mu\boldsymbol{\varphi}$, where $K = (K_{ij}) \in \mathbb{R}^{N \times N}$. Under our assumptions, the weight w_j does not depend on j, which makes K symmetric.

Outline

Outline

Image Approximation; Comparison with Wavelets

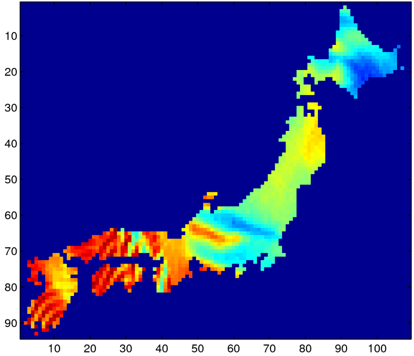

(a) What data?

Image Approximation; Comparison with Wavelets

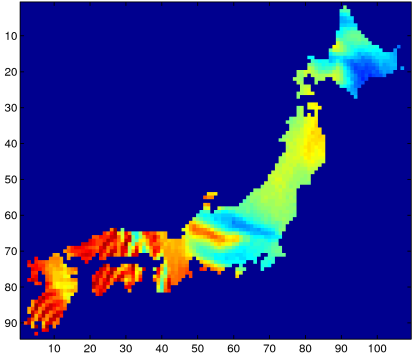

(a) What data?

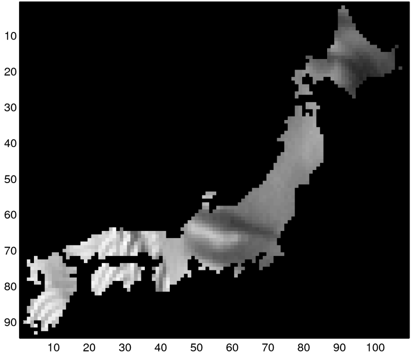

(b) $\chi_J \cdot$ Barbara

First 25 Basis Functions

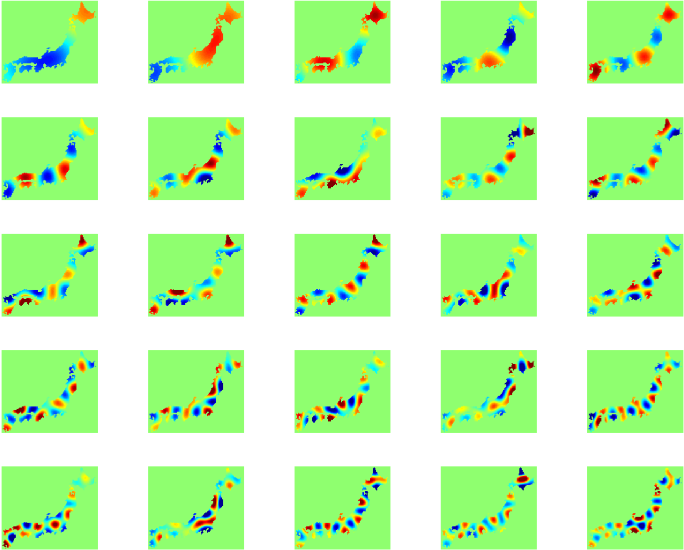

Next 25 Basis Functions

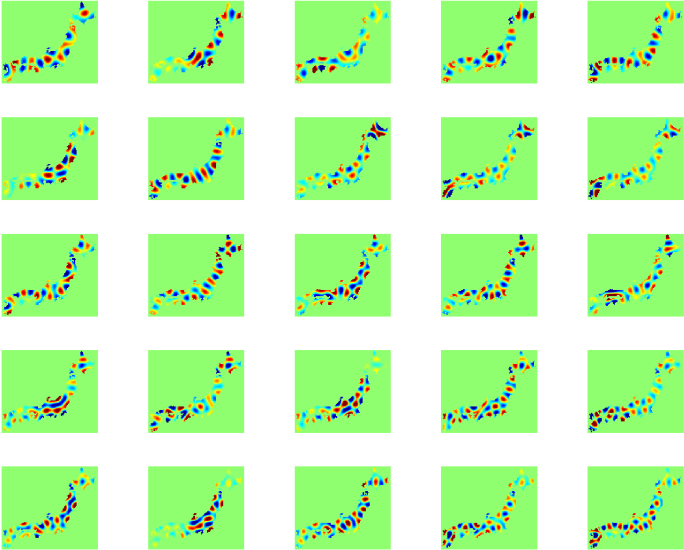

Reconstruction with Top 100 Coefficients

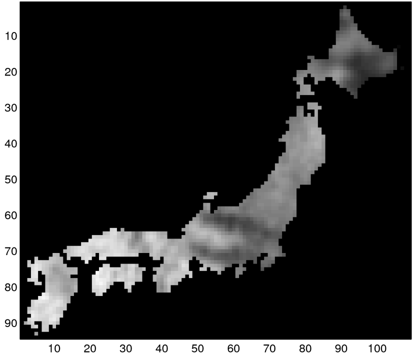

(a) Reconstruction

Reconstruction with Top 100 Coefficients

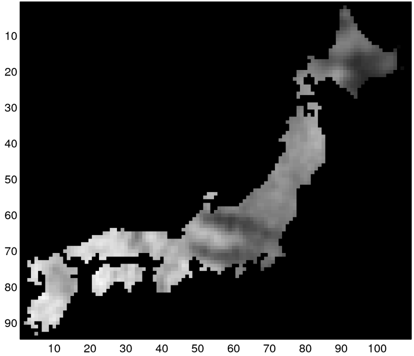

(a) Reconstruction

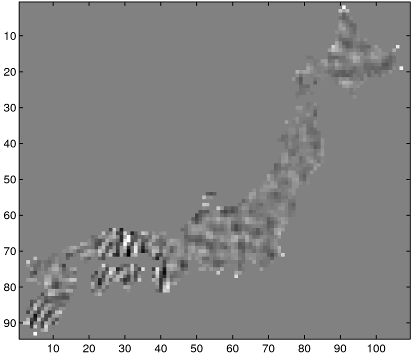

(b) Error

Reconstruction with Top 100 2D Wavelets (Symmlet 8)

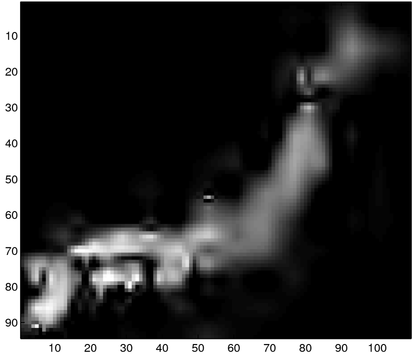

(a) Reconstruction

Reconstruction with Top 100 2D Wavelets (Symmlet 8)

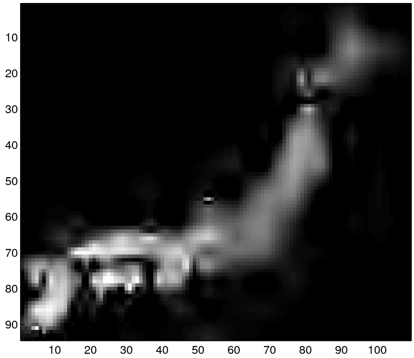

(a) Reconstruction

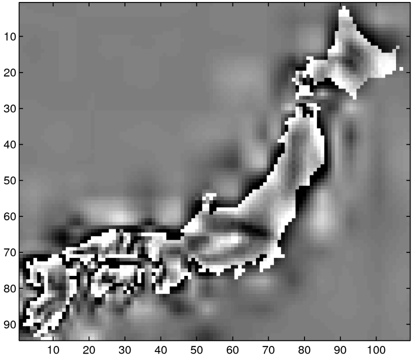

(b) Error

Reconstruction with Top 100 1D Wavelets (Symmlet 8)

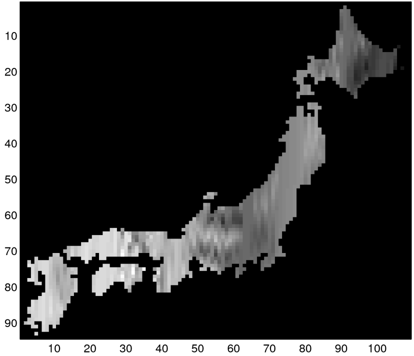

(a) Reconstruction

Reconstruction with Top 100 1D Wavelets (Symmlet 8)

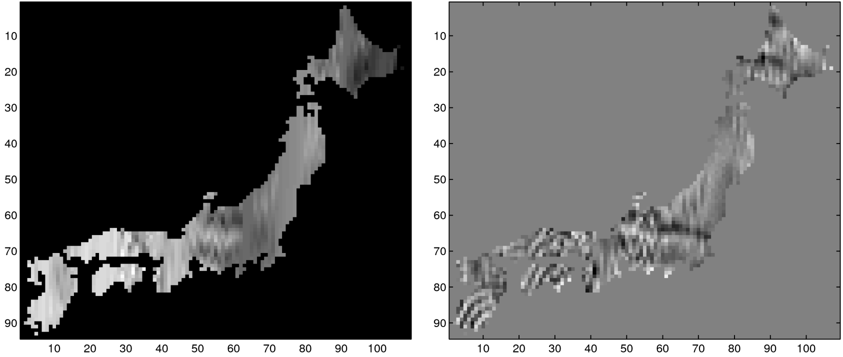

(a) Reconstruction (b) Error

Comparison of Coefficient Decay

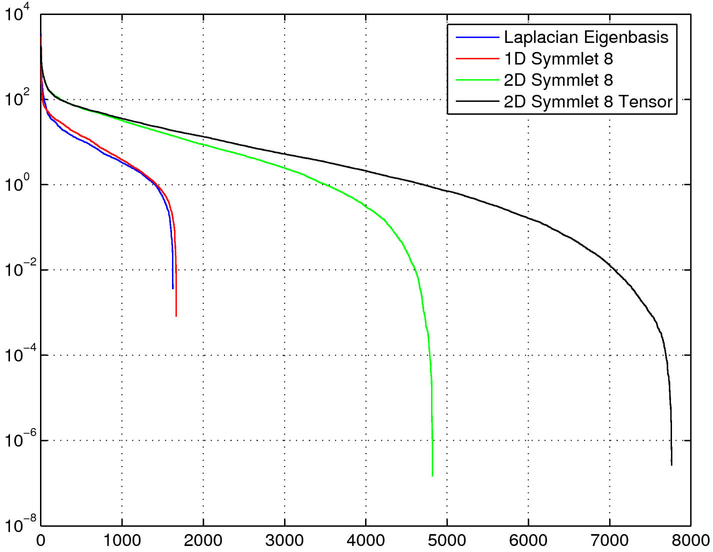

A Real Challenge: Kernel matrix is of 387924 × 387924.

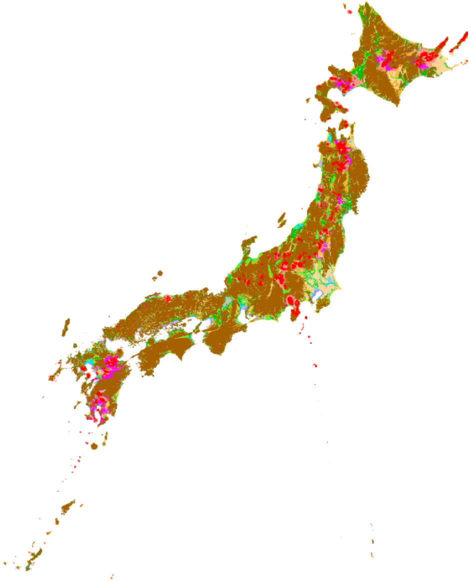

First 25 Basis Functions via the FMM-based algorithm

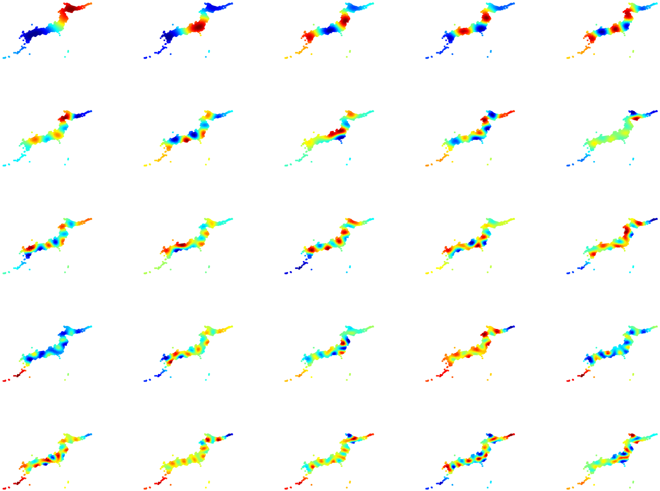

Outline

Experiments on Domains with Perturbed Boundaries

We will use the following domains for our experiments:

Ω_1: The Japanese Islands

Ω_2: A smoothed and connected version of Ω_1;

Ω_3: The same as Ω_2 but with a "jaggy" boundary curve

Ω_4: The two-component version of Ω_2.

As for the data on these domains, we adopted three functions with different smoothness:

1. A discontinuous function (i.e., a simple step function whose discontinuity is a straight line along the "spine" or the main axis of the domain);
2. A pyramid-shaped function, which is continuous and its first order partial derivatives are of bounded variation;
3. The standard Gaussian function.

The Domains with Perturbed Boundaries

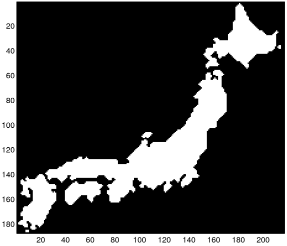

(a) χ_{Ω_1}

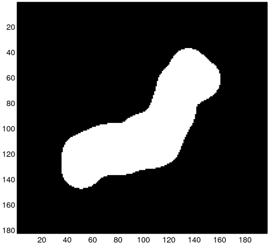

(b) χ_{Ω_2}

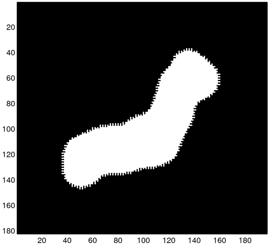

(c) χ_{Ω_3}

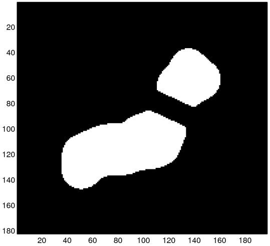

(d) χ_{Ω_4}

Decay Rates of the Expansion Coefficients (Unsorted)

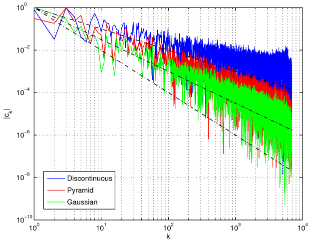

(a) Decay rates on Ω_1

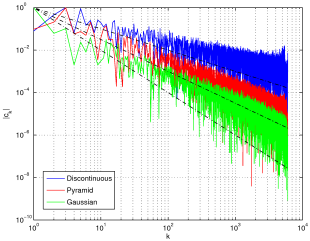

(b) Decay rates on Ω_2

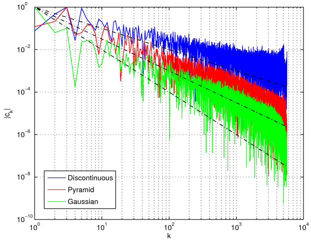

(c) Decay rates on Ω_3

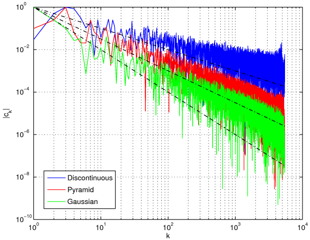

(d) Decay rates on Ω_4

Observations on the Decay Rates

- The decay rates reflect the intrinsic smoothness of the functions living in the domain, but are not affected by the existence of the boundary of the domains.
- The decay rates are rather insensitive to the smoothness of the boundary curves. In particular, the plots for Ω_2, Ω_3, and Ω_4 are virtually the same whereas those for Ω_1—the most complicated domain among these four—seem slightly worse than the others. Yet all behave better than $O(k^{-1})$.
- The decay rates are rather insensitive to the number of the separated subdomains. Again, it will be also of interest to investigate the behavior the conventional Laplacian eigenfunctions in this respect.
- Although the coefficient plots oscillate around the linear lines (in the log-log scale), the decay rates $O(k^{-\alpha})$, regardless of the domain shapes, behave as follows. For the discontinuous functions, $\alpha < 1$. For the pyramid-shape function, $1 < \alpha < 1.5$. For the Gaussian function, $\alpha \geq 1.5$.

Decay Rates of the Expansion Coefficients (Sorted)

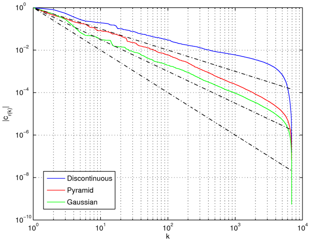

(a) Decay rates on Ω_1

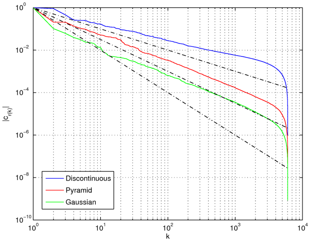

(b) Decay rates on Ω_2

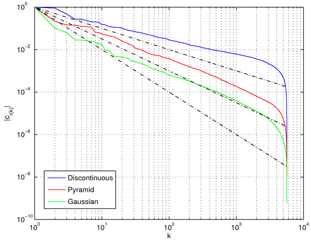

(c) Decay rates on Ω_3

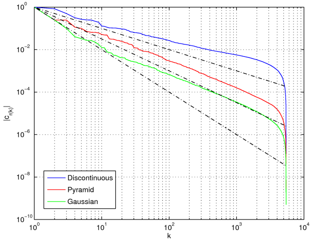

(d) Decay rates on Ω_4

Conjecture on the Coefficient Decay Rate

Conjecture (NS 2007)

Let Ω be a C^2-domain of general shape and let $f \in C\left(\overline{\Omega}\right)$ with $\dfrac{\partial f}{\partial x_j} \in BV\left(\overline{\Omega}\right)$ for $j = 1, \ldots, d$. Let $\{c_k = \langle f, \phi_k \rangle\}_{k \in \mathbb{N}}$ be the expansion coefficients of f with respect to our Laplacian eigenbasis on this domain. Then, $|c_k|$ decays with rate $O(k^{-\alpha})$ with $1 < \alpha < 2$ as $k \to \infty$. Thus, the approximation error using the first m terms measured in the L^2-norm, i.e., $\|f - \sum_{k=1}^{m} c_k \phi_k\|_{L^2(\Omega)}$ should have a decay rate of $O(m^{-\alpha+0.5})$ as $m \to \infty$.

Outline

Image Extrapolation

- Recall the definition of the eigenvalue problem:

$$\varphi(\mathbf{x}) = \frac{1}{\mu}\int_\Omega K(\mathbf{x},\mathbf{y})\varphi(\mathbf{y})\,\mathrm{d}\mathbf{y}, \quad \text{where } \mathbf{x} \text{ can be any point in } \mathbb{R}^d.$$

- For large μ (i.e., coarse scale/low frequency), extrapolation naturally extends to large area.
- For small μ (i.e., fine scale/high frequency), extrapolation quickly attenuates away from Ω.

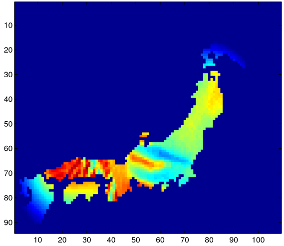

Figure: Extrapolation of χ_{Honshu}. Barbara to the three islands.

Outline

Hippocampal Shape Analysis

- Presenting the work of Faisal Beg and his group at Simon Fraser Univ. using our technique
- Want to distinguish people with mild dementia of the Alzheimer type (DAT) from cognitively normal (CN) people
- Hippocampus plays important roles in long-term memory and spatial navigation

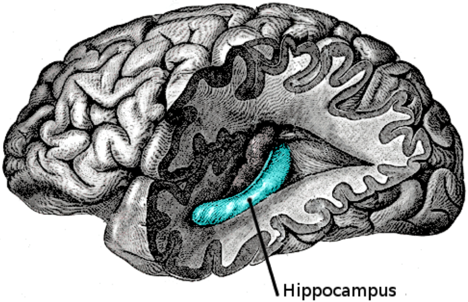

Figure: From Wikipedia

- Dataset: Left hippocampus segmented from 3D MRI images
- Compute the smallest 999 Laplacian eigenvalues (i.e., the largest 999 eigenvalues of the integral operator $\mathcal{K}$) for each left hippocampus
- Construct a feature vector for each left hippocampus:

$$\mathbf{F} \triangleq \left(\frac{\lambda_1}{\lambda_2}, \ldots, \frac{\lambda_1}{\lambda_{n+1}} \right)^T = \left(\frac{\mu_2}{\mu_1}, \ldots, \frac{\mu_{n+1}}{\mu_1} \right)^T \in \mathbb{R}^n.$$

  This feature vector was used by Khabou, Hermi, and Rhouma (2007) for 2D shape classification (e.g., shapes of tree leaves).
- Reduce the feature space dimension via PCA to from $n = 998$ to n'
- Classified by the linear SVM (support vector machine)

Hippocampal Image Analysis . . .

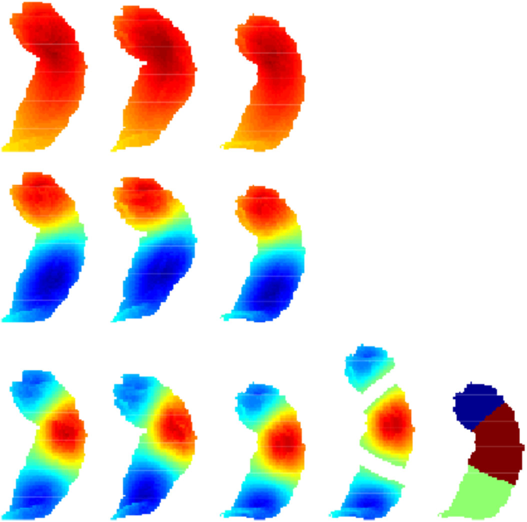

Spectral Geometry 101

- The Laplacian eigenfunctions defined on the domain Ω provides the orthonormal basis of $L^2(\Omega)$.
- The Laplacian eigenvalues encode geometric information of the domain $\Omega \Longrightarrow$ "Can we hear the shape of a drum?" (Mark Kac, 1966).
- Temporarily, consider the Laplacian eigenvalue problem on a planar domain $\Omega \in \mathbb{R}^2$ with the Dirichlet boundary condition:

$$\begin{cases} -\Delta u = \lambda u & \text{in } \Omega \\ u = 0 & \text{on } \partial\Omega. \end{cases}$$

- Let $0 < \lambda_1 \leq \lambda_2 \leq \lambda_3 \leq \cdots \leq \lambda_k \leq \cdots \to \infty$ be the sequence of eigenvalues of the above Dirichlet-Laplace eigenvalue problem.
- Kac showed (based on the work of Weyl, Minakshisundaram-Pleijel):

$$\sum_{k=1}^{\infty} \mathrm{e}^{-\lambda_k t} = \frac{|\Omega|}{4\pi t} - \frac{|\partial\Omega|}{8\sqrt{\pi t}} + o(t^{-1/2}) \quad \text{as } t \downarrow 0.$$

Universal (or Payne-Pólya-Weinberger) Inequalities

For $m = 1, 2, \dots$

- $\lambda_{m+1} - \lambda_m \leq 2 \cdot \frac{1}{m} \sum_{j=1}^{m} \lambda_j.$
- $\frac{\lambda_{m+1}}{\lambda_m} \leq 3.$
- $\sum_{j=1}^{m} \frac{\lambda_j}{\lambda_{m+1} - \lambda_j} \geq \frac{m}{2}$ (Hile-Protter).
- $\sum_{j=1}^{m} (\lambda_{m+1} - \lambda_j)^2 \leq 2 \sum_{j=1}^{m} \lambda_j (\lambda_{m+1} - \lambda_j)$ (Yang).
- $\lambda_{m+1} \leq 3 \cdot \frac{1}{m} \sum_{j=1}^{m} \lambda_j.$

Isoperimetric Inequalities

- $\lambda_1 \geq \dfrac{\pi^2 j_{0,1}^2}{|\Omega|^2}$ (Faber-Krahn)
- $\dfrac{\lambda_2}{\lambda_1} \leq \dfrac{j_{1,1}^2}{j_{0,1}^2} \approx 2.5387$ (Ashbaugh-Benguria)
- $j_{k,1}$ is the first zero of the Bessel function of order k, i.e., $J_k(j_{k,1}) = 0$. $j_{0,1} \approx 2.4048$, $j_{1,1} \approx 3.8317$, and $|\Omega|$ is the area of Ω. In both cases, the equality is attained iff Ω is a disk in $\mathbb{R}^2$.

Other Properties

- Domain monotonicity property:

$$\Omega_1 \subset \Omega_2 \Longrightarrow \lambda_k(\Omega_1) \geq \lambda_k(\Omega_2), \quad k \in \mathbb{N}.$$

- Scaling property:

$$\lambda_k(\alpha\,\Omega) = \frac{\lambda_k(\Omega)}{\alpha^2}, \quad \alpha > 0,\ k \in \mathbb{N}.$$

  This implies:

$$\frac{\lambda_k(\alpha\,\Omega)}{\lambda_m(\alpha\,\Omega)} = \frac{\lambda_k(\Omega)}{\lambda_m(\Omega)}, \quad k,\ m \in \mathbb{N}.$$

  $\Longrightarrow$ the ratios of Laplacian eigenvalues are scale invariant.

- Laplacian eigenvalues are translation and rotation invariant.
- See also "Shape DNA" by Reuter et al. (2005), and classification of tree leaves by Khabou et al. (2007).
- Some properties and inequalities listed above should hold not only for the Dirichlet Laplacian eigenvalues but also for our Laplacian eigenvalues. Note, however, that the domain monotonicity does not hold for the Neumann Laplacian eigenvalues.

Hippocampal Shape Analysis: φ_2

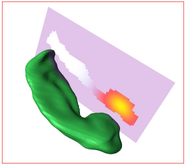

(a) $N = 15135$

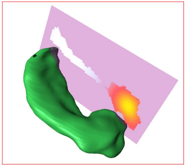

(b) $N = 15438$

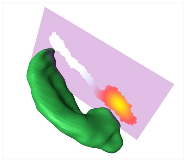

(c) $N = 14938$

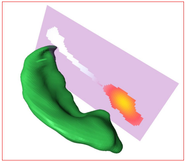

(d) $N = 15256$

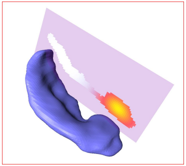

(e) $N = 14201$

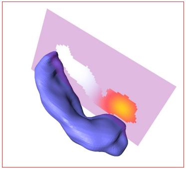

(f) $N = 15630$

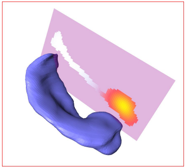

(g) $N = 12073$

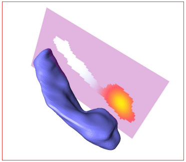

(h) $N = 12240$

Hippocampal Shape Analysis: φ_3

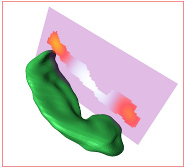

(i) $N = 15135$

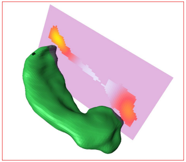

(j) $N = 15438$

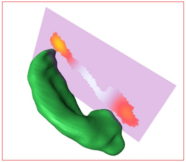

(k) $N = 14938$

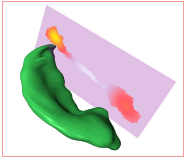

(l) $N = 15256$

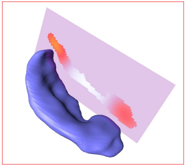

(m) $N = 14201$

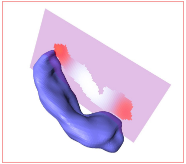

(n) $N = 15630$

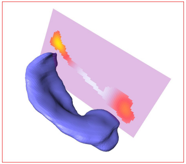

(o) $N = 12073$

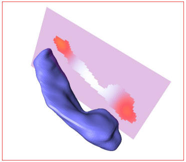

(p) $N = 12240$

Hippocampal Shape Analysis . . .

- Dataset consists of the segmented left hippocampuses of 18 DAT subjects and of 26 CN subjects

Method	Accuracy	Specificity	Sensitivity	n	n'
MomInv	68.1%	69.2%	66.6%	12	1
TensorInv	75.0%	76.9%	72.2%	$\geq 1.9E5$	17
LapEig	77.2%	84.6%	66.6%	998	14
GeodesicInv	86.3%	77.7%	92.3%	$\geq 1.3E6$	27

$$\text{accuracy} \triangleq \frac{|TP| + |TN|}{|\text{people examined}|} = \frac{|\text{people correctly diagnosed}|}{|\text{people examined}|}$$

$$\text{specificity} \triangleq \frac{|TN|}{|TN| + |FP|} = \frac{|\text{people correctly diagnosed as healthy}|}{|\text{healthy people examined}|}$$

$$\text{sensitivity} \triangleq \frac{|TP|}{|TP| + |FN|} = \frac{|\text{people correctly diagnosed as mild AD}|}{|\text{people with mild AD examined}|}$$

Outline

Comparison with PCA

- Consider a stochastic process living on a domain Ω.
- PCA/Karhunen-Loève Transform is often used.
- PCA/KLT incorporate geometric information of the measurement (or pixel) location through the data correlation, i.e., implicitly.
- Our Laplacian eigenfunctions use explicit geometric information through the harmonic kernel $K(\mathbf{x}, \mathbf{y})$.

Comparison with PCA: Example

- *"Rogue's Gallery"* dataset from Larry Sirovich
- 72 training dataset; 71 test dataset
- Left & right eye regions

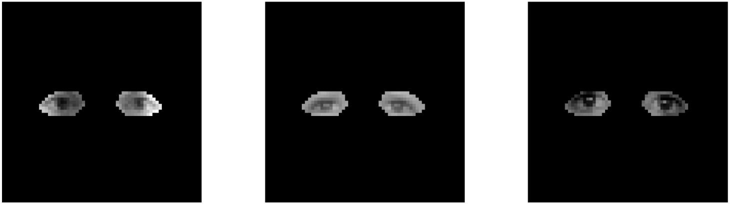

Comparison with PCA: Basis Vectors

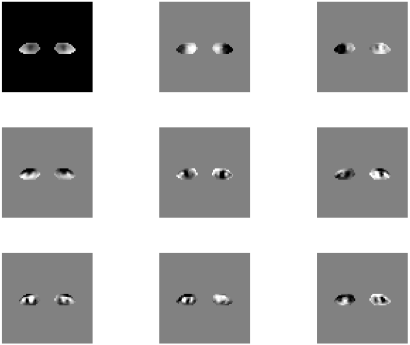

(a) KLB/PCA 1:9

Comparison with PCA: Basis Vectors

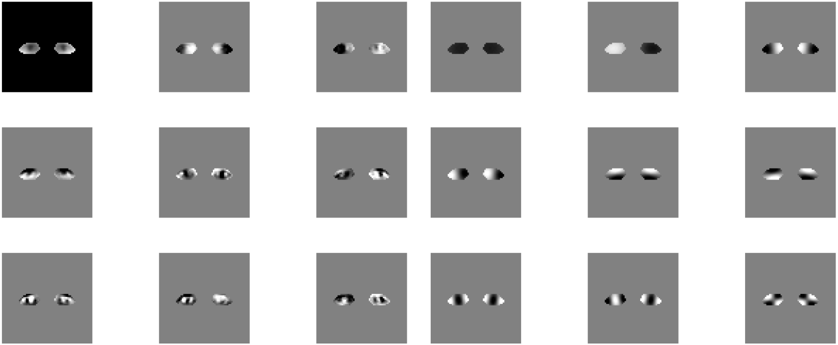

(a) KLB/PCA 1:9 (b) Laplacian Eigenfunctions 1:9

Comparison with PCA: Basis Vectors . . .

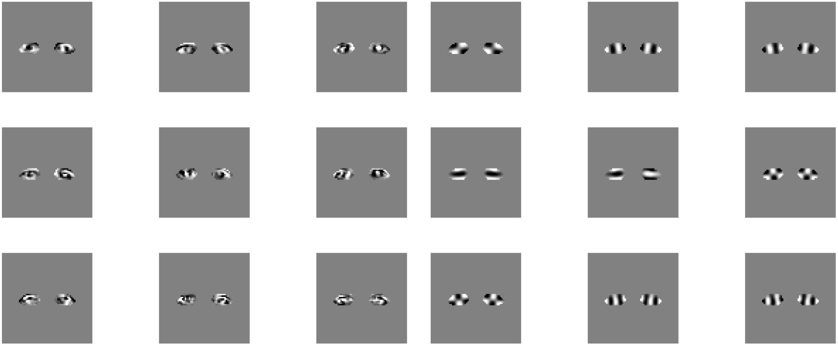

(a) KLB/PCA 10:18 (b) Laplacian Eigenfunctions 10:18

Comparison with PCA: Kernel Matrix

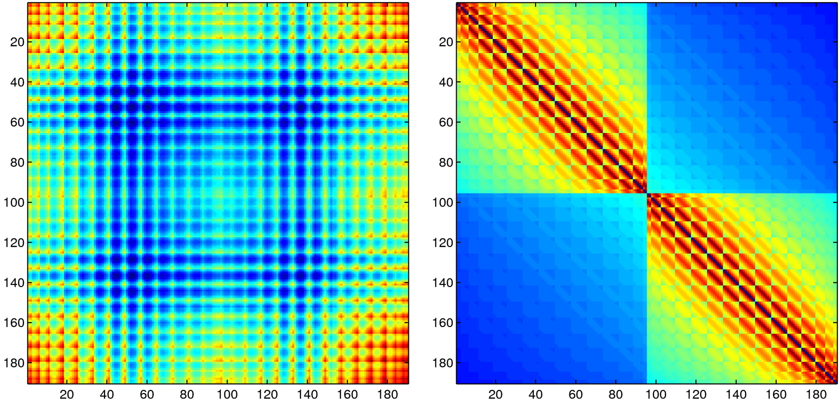

(a) Covariance (b) Harmonic kernel

Comparison with PCA: Energy Distribution over Coordinates

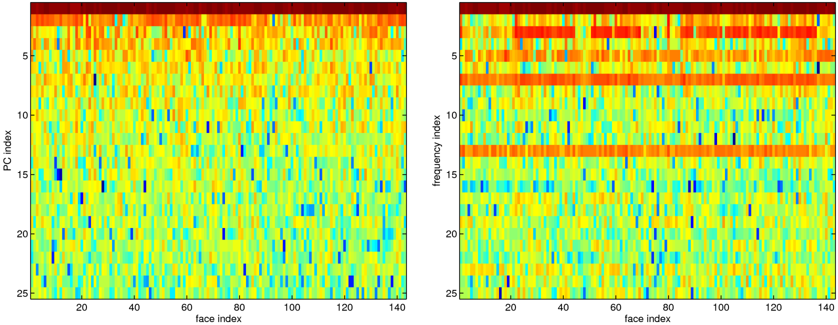

(a) KLB/PCA

(b) Laplacian Eigenfunctions

Comparison with PCA: Basis Vector #7 . . .

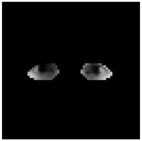

c_7:large

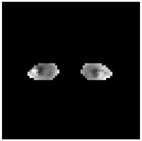

c_7:large

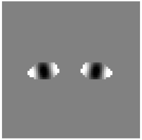

φ_7

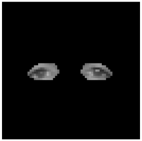

c_7:small

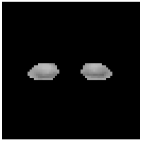

c_7:small

Comparison with PCA: Basis Vector #13 . . .

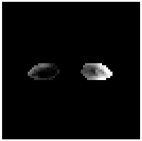

c_{13}:large

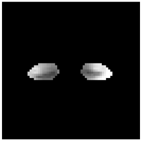

c_{13}:large

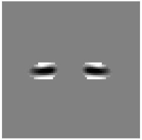

φ_{13}

c_{13}:small

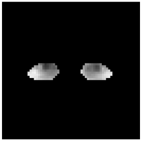

c_{13}:small

Asymmetry Detector

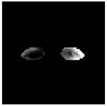

Eyes #80

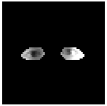

Eyes #22

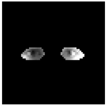

Eyes #52

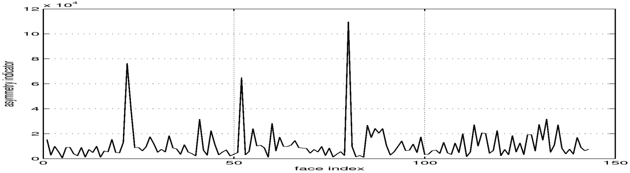

Asymmetry detector

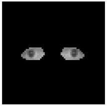

Eyes #5

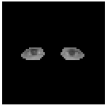

Eyes #84

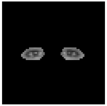

Eyes #59

Outline

A Possible Fast Algorithm for Computing φ_j's

- Observation: our kernel function $K(\mathbf{x}, \mathbf{y})$ is of special form, i.e., the fundamental solution of Laplacian used in potential theory.
- Idea: Accelerate the matrix-vector product $K\varphi$ using the Fast Multipole Method (FMM).
- Convert the kernel matrix to the tree-structured matrix via the FMM whose submatrices are nicely organized in terms of their ranks. (Computational cost: our current implementation costs $O(N^2)$, but can achieve $O(N \log N)$ via the randomized SVD algorithm of Woolfe-Liberty-Rokhlin-Tygert (2008)).
- Construct $O(N)$ matrix-vector product module fully utilizing rank information (See also the work of Bremer (2007) and the "HSS" algorithm of Chandrasekaran et al. (2006)).
- Embed that matrix-vector product module in the Krylov subspace method, e.g., Lanczos iteration.
  (Computational cost: $O(N)$ for each eigenvalue/eigenvector).

Tree-Structured Matrix via FMM

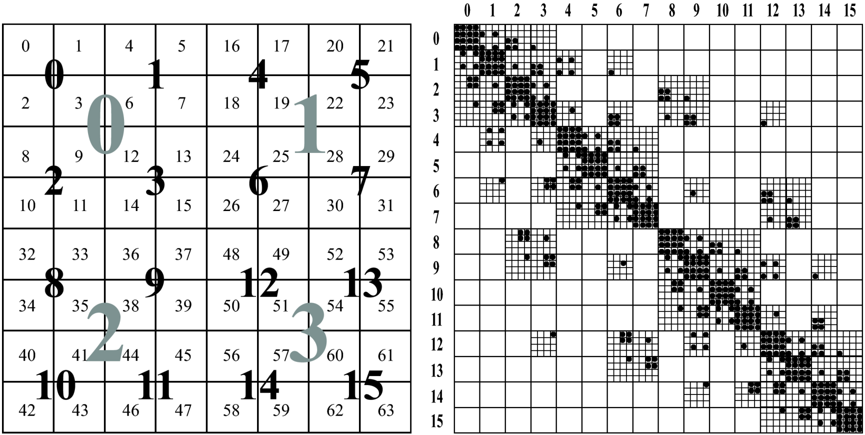

(a) Hierarchical indexing scheme (b) Tree-Structured Matrix

First 25 Basis Functions via the FMM-based algorithm

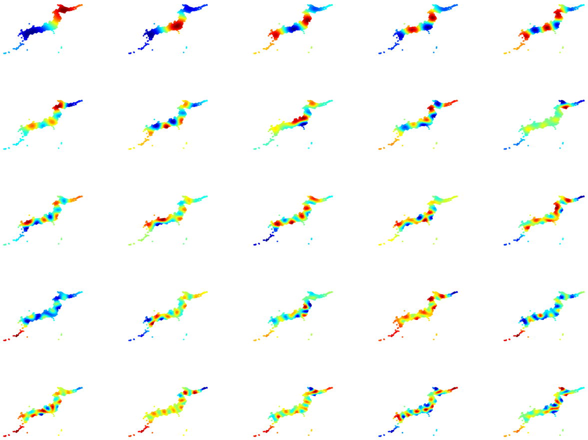

Splitting into Subproblems for Faster Computation

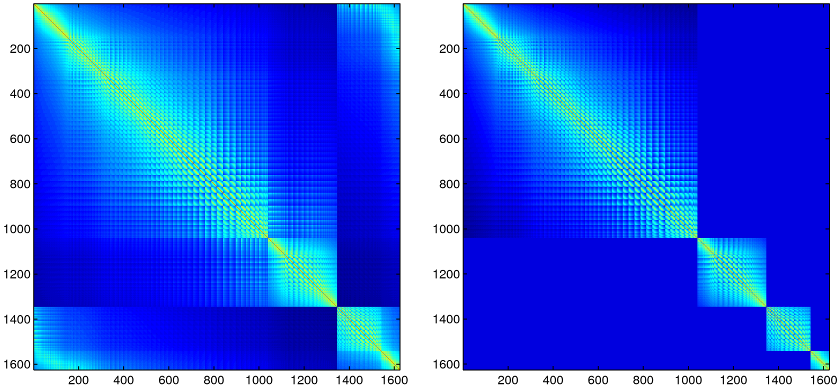

(a) Whole islands (b) Separated islands

Eigenfunctions for Separated Islands

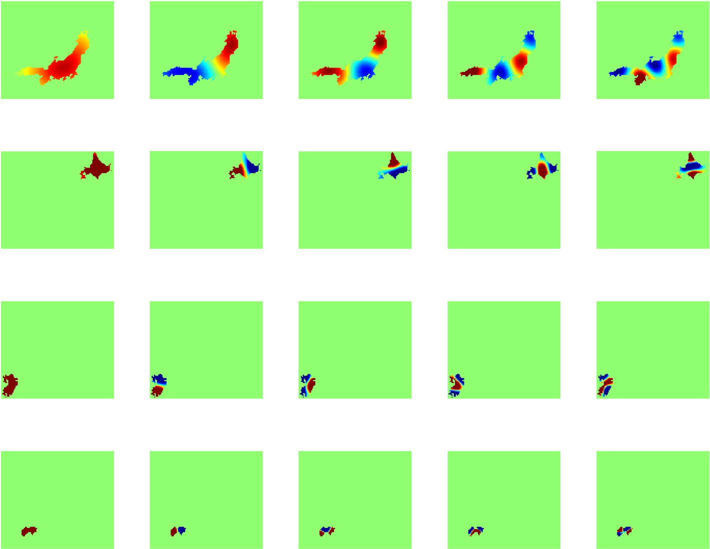

Outline

Conclusions

- Allow object-oriented image analysis & synthesis
- Can get fast-decaying expansion coefficients
- Can decouple geometry/domain information and statistics of data
- Can extract geometric information of a domain through the eigenvalues
- $\exists$ A variety of applications: interpolation, extrapolation, local feature computation, solving heat equations on complicated domains ...
- Fast algorithms are the key for higher dimensions/large domains
- Connection to lots of interesting mathematics: spectral geometry, spectral graph theory, isoperimetric inequalities, Toeplitz operators, PDEs, potential theory, almost-periodic functions, ...
- Many things to be done:
  - Asymptotic theory for various spectral functions, $Z(t) = \sum \mathrm{e}^{-\lambda_k t}$, $\zeta(t) = \sum \frac{1}{\lambda_k^t}$, $N(z) = \sum_{\lambda_k \leq z} 1$, $C(z) = \sum_{\lambda_k \leq z} \frac{1}{\lambda_k}$, etc.
  - How about higher order, i.e., polyharmonic ?
  - Features derived from heat kernels ?
  - Improve our fast algorithm

Outline

References

- Laplacian Eigenfunction Resource Page http://www.math.ucdavis.edu/~saito/lapeig/ contains
  - My Course Note (elementary) on "Laplacian Eigenfunctions: Theory, Applications, and Computations"
  - All the talk slides of the minisymposia on Laplacian Eigenfunctions at ICIAM 2007, Zürich (Organizers: NS, Mauro Maggioni), and at SIAM Imaging Science Conference 2008, San Diego (Organizers: NS, Xiaomin Huo)
  - A link to a short IPAM program (5 days) on "Laplacian Eigenvalues and Eigenfunctions: Theory, Computation, Application" Feb. 2009.
- The following article is available at http://www.math.ucdavis.edu/~saito/publications/
  - N. Saito: "Data analysis and representation using eigenfunctions of Laplacian on a general domain," *Applied & Computational Harmonic Analysis*, vol. 25, no. 1, pp. 68–97, 2008.

Thank you very much for your attention!